Acta Geochim (2023) 42:739–746
https://doi.org/10.1007/s11631-023-00605-x

ORIGINAL ARTICLE

Europium anomalies in detrital zircons reveal the crustal thickness evolution of South China in Early Neoproterozoic

Zhi Chen[1]

Received: 4 January 2023 / Revised: 20 March 2023 / Accepted: 20 March 2023 / Published online: 24 April 2023

Abstract The South China Block (SCB) is formed by the amalgamation of the Yangtze and Cathaysia blocks during the Early Neoproterozoic along the Jiangnan Orogen. However, the precise amalgamation time of these two blocks and the location of the united SCB in the Rodinia supercontinent remain highly debatable. Various tectonic models have been proposed and they may have different implications for the crustal thickness evolution of the central SCB in Early Neoproterozoic. To evaluate these models, this paper uses a recently calibrated Eu/Eu*-in-zircon proxy to reconstruct crustal thickness evolution of the central SCB during Early Neoproterozoic. I compiled and screened U–Pb ages and trace elements of 900–700 Ma detrital zircons from the central SCB and then calculated the zircon Eu/Eu* values. The age-binned average zircon Eu/Eu* displays a decreasing trend from 870 to 790 Ma, and thus indicates no significant crustal thickening event occurred during this time interval. This finding seems to be inconsistent with tectonic models that the Yangtze and Cathaysia blocks amalgamated during this time interval. Yet, given that available coupled detrital zircon U–Pb and trace element datasets are very limited, additional studies are warranted to further evaluate this hypothesis.

Keywords South China · Crustal thickness · Neoproterozoic · Detrital zircon · Eu anomalies

✉ Zhi Chen
zhichen@nigpas.ac.cn

[1] Nanjing Institute of Geology and Palaeontology, Chinese Academy of Sciences, Nanjing, China

1 Introduction

The South China Block (SCB), one of the largest continental blocks in East Asia, was formed by the amalgamation of the Yangtze Block in the northwest and the Cathaysia Block in the southeast (modern coordinates, Fig. 1) along the Jiangnan orogen (also referred to as "Sibao" or "Jinning" orogen in the literature) during Neoproterozoic (Cawood et al. 2020; Charvet 2013; Li et al. 2008a, b, 2009; Shu et al. 2021; Zhao and Cawood 2012; Zhou et al. 2002). The assemblage of the unified SCB is thought to be related to the evolution of the Neoproterozoic supercontinent Rodinia as the SCB is widely accepted as an integral part of the supercontinent (Li et al. 2008a, b). However, controversies exist regarding the exact timing of the amalgamation between the Yangtze and Cathaysia blocks and the precise position of SCB in the Rodinia, although extensive structural, metamorphic, stratigraphic, petrological, geochronological, geochemical, and geophysical studies have been carried out (Li et al. 2008a, b, 2009, 2010; Lu et al. 2022; Park et al. 2021; Shu et al. 2021; Wang and Li 2003; Wang et al. 2012, 2014; Yang et al. 2015; Yao et al. 2021; Zheng et al. 2008; Zhou et al. 2002). There are two major viewpoints regarding these two related questions. One school of researchers believed that the amalgamation between the Yangtze and Cathaysia blocks took place at ca. 1.0–0.9 Ga (Li et al. 2008a, b, 2009, 2010; Yang et al. 2015) as a part of the worldwide Grenvillian-aged orogenic events associated with the assemblage of Rodinia, and the SCB occupied an internal position within the supercontinent (Li et al. 2002, 2008a, b). The other group of researchers argued that the Yangtze–Cathaysia amalgamation occurred at ca. 0.82 Ga, significantly later than the global Grenville orogeny,

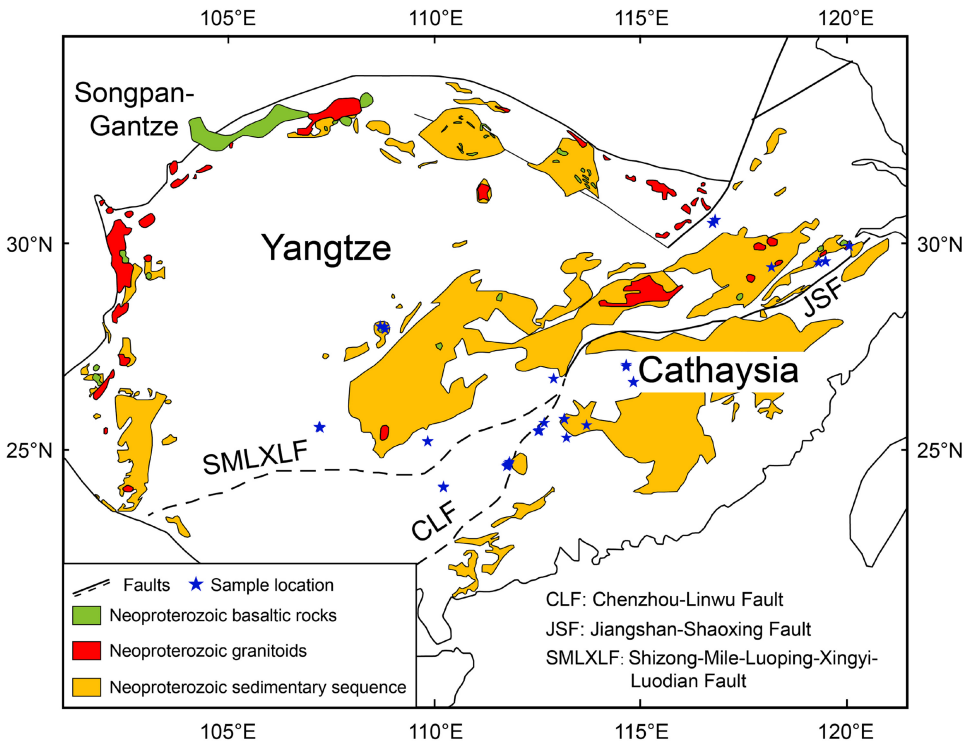

Fig. 1 Simplified geological map of South China block showing major Neoproterozoic units and faults (modified after Yang et al. 2016)

and the SCB occupied a peripheral location in the Rodinia (Cawood et al. 2020; Shu et al. 2021; Wang et al. 2019; Xu et al. 2014; Zhang et al. 2012; Zhao et al. 2011). These two tectonic models may correspond to different crustal thickness evolution of central SCB during the Neoproterozoic period.

Recent studies found that europium anomalies [Eu/Eu*; chondrite normalized Eu $= \sqrt{(\mathrm{Sm} \times \mathrm{Gd})}$] in detrital zircons can be used to reconstruct crustal thickness evolution (Tang et al. 2021a, b). Uniquely among the REE, which are usually trivalent (except Ce), Eu can exist as both a divalent cation (Eu^{2+}) and a trivalent cation (Eu^{3+}). Eu^{2+} is preferentially incorporated into the Ca^{2+} site of plagioclase, whereas it is less compatible in zircon than Eu^{3+} as the size and charge of Eu^{2+} are more different from Zr^{4+} than those of Eu^{3+} (Burnham and Berry 2012; Hoskin and Schaltegger 2003; Loader et al. 2017; Viala and Hattori 2021). Thus, zircon Eu anomaly is influenced by the magmatic oxidation state and the plagioclase fractional crystallization or residual (Hoskin and Schaltegger 2003; Kong 2022; Loader et al. 2017; Trail et al. 2012). Intense crustal thickening destabilizes plagioclase and stabilizes garnet, the latter of which increases the Fe^{3+}/Fe_T ratio (ferric Fe to total Fe ratio, $Fe_T = Fe^{3+} + Fe^{2+}$) of the residual melt as garnet prefers ferrous (Fe^{2+}) over ferric ion (Fe^{3+}) (Tang et al. 2019, 2021b). The elevated Fe^{3+}/Fe_T would then oxidize Eu^{2+} and enhance Eu partitioning in zircon (Tang et al. 2021b). The collective effect is that zircon Eu/Eu* positively correlates with crustal thickness.

In this contribution, I compile Early Neoproterozoic detrital zircon U–Pb geochronological and trace element data along Jiangnan orogen in an attempt to advance the debate on the timing of amalgamation between the Yangzte and Cathaysia blocks and evaluate the various proposed models for the assemblage of SCB using recently calibrated Eu/Eu*-in-zircon crustal thickness proxy.

2 Geological background

The SCB is separated from the North China Craton to the north by the Qinling–Dabie–Sulu orogenic belt, from the Songpan–Gantze terrane to the northwest by the Longmenshan Fault, from the Indochina Block to the southwest by the Ailaoshan–Song Ma suture zone and is bounded to the southeast by the Pacific Ocean but extends beyond the Chinese mainland (Fig. 1). The SCB is composed of the Yangtze Block in the northwest and the Cathaysia Block in the southeast which were sutured together along the Jiangnan Orogen during the Neoproterozoic, although the specific timing of the collision between these two blocks is still controversial (Li et al. 2008a, b; Shu et al. 2019; Zhao et al. 2011). The Jiangnan orogen is a NE-SW trending mobile belt through the middle of SCB, with a width of $\sim$ 120 km and a length of $\sim$ 1500 km, which extends from southern Anhui and western Zhejiang provinces in the east, through northern Jiangxi in the center, to eastern Guizhou, northern Guangxi, and western Hunan in the west

(Kou et al. 2018). Generally, the boundary between Yangtze and Cathaysia blocks in the northeast is considered to be the Jiangshan–Shaoxing Fault, whereas the boundary in the southwest is still disputed (Guo and Gao 2018; Shu et al. 2019; Zhao and Cawood 2012).

Shortly after the amalgamation of the Yangtze and Cathaysia blocks, the unified SCB experienced intense rifting along the Jiangnan orogen in the Neoproterozoic, resulting in the formation of an intracontinental Nanhua rift basin between the Yangtze and Cathaysia blocks (Li et al. 2010). This rift basin hosted thick Neoproterozoic sedimentary successions consisting of several major unconformity-bounded sequence-sets (Wang and Li 2003) and was succeeded by a foreland basin during the Ediacaran-Early Paleozoic (Yao et al. 2015). Early Neoproterozoic granites and volcanic rocks are widespread in the SCB, especially around the periphery of the Yangtze Block (Lyu et al. 2017; Zhao et al. 2018). They are the major sources of the Neoproterozoic detrital zircons in the central SCB (Wang et al. 2012; Yang et al. 2015; Yao et al. 2012).

3 Methods and data compilation

The $[La/Yb]_N$ (the subscript N means chondrite normalized) ratios of magmatic rocks have been found to positively correlate with crustal thickness (Hu et al. 2017, 2020; Profeta et al. 2015). This geochemical discrimination is possible due to the different affinity of these rare earth elements to garnet and/or amphibole. At higher pressure or greater depth, heavy rare earth elements HREEs (e.g., Yb) are preferentially incorporated into garnet and/or amphibole, whereas light rare earth elements LREEs (e.g., La) readily enter the liquid phase, leading to high La/Yb ratios. In contrast, at lower pressure or depth, HREEs preferentially partition into the liquid phase, resulting in low La/Yb ratios. Therefore, larger whole rock La/Yb ratios signify rocks formed at higher pressures and greater depths, and thus within thicker crust (Hu et al. 2017; Lieu and Stern 2019; Profeta et al. 2015). Consequently, La/Yb ratios in magmatic rocks are often used to quantitate the average crustal pressure and the corresponding depth at which rocks are formed (Hu et al. 2017; León et al. 2021; Wang et al. 2022; Zeng et al. 2022; Zhu et al. 2017).

However, for deep time, its application to estimate crustal thickness is limited by the increasingly significant issue of preservation of rock records, because this whole rock chemistry method requires extensive sampling over large areas in the field. Tang et al. (2021b) found that within intermediate to felsic rocks, the amplitude of Eu anomalies in detrital zircons correlates with the whole rock La/Yb ratios. Eu anomalies in detrital zircons have been used to calculate crustal thickness (Carrapa et al. 2022; Tang et al. 2021a; Zeng et al. 2022). The zircon-based crustal thickness proxy may be a more convenient paleomohometric tool than the whole-rock approach, which can extract information about orogen-wide patterns from just a few batches of carefully targeted zircon-bearing sedimentary rocks (Luffi and Ducea 2022). Another advantage of Eu/Eu*-in-zircon proxy is that zircon is a ubiquitous mineral and can survive most erosion and weathering processes. Not only are zircons exceptionally well preserved in sedimentary rocks and carry age information for the original magmatic sources, but zircons preserved in the detrital archive can span almost the entire range of Earth's age, which can fill gaps in Earth's history where rock records are missing and provide a continuous record of crustal thickness evolution (Tang et al. 2021b).

In this study, to test the tectonic models of the amalgamation between the Yangtze and Cathayia blocks, I use the Eu anomaly proxy of the detrital zircons as a senor for crustal thickness evolution from 900 to 700 Ma. I compiled previously published detrital zircon U–Pb age data with trace element concentration analyses conducted on the same individual grains from central SCB and their P contents (if available) (Jiang et al. 2019, 2020; Meng et al. 2015; Qi et al. 2021; Song et al. 2020; Wu et al. 2018; Xiong et al. 2019; Xu et al. 2018; Yao et al. 2012; Zhang et al. 2015, 2016, 2019). Only zircon ages that are within 90%–110% of concordance [$100 \times (^{206}Pb/^{238}U$ age/$^{207}Pb/^{206}Pb$ age)] were accepted and $^{206}Pb/^{238}U$ ages were used as their crystallization ages. The compilation contains 685 geochronological and trace element analyses of detrital zircon grains whose ages range from 900 to 700 Ma. Compiled data were further filtered using the methods of Tang et al. (2021a, b) and Zhu et al. (2020) before applying the Eu/Eu*-in-zircon crustal thickness proxy. The Neoproterozoic granites in central SCB can be divided into three distinct groups, namely I-type (igneous protoliths), S-type (sedimentary protoliths), and A-type (shallow emplacement) granitoid. I-type and A-type samples show a positive correlation between zircon Eu/Eu* and whole rock $[La/Yb]_N$, while zircon Eu/Eu* does not correlate with the whole rock $[La/Yb]_N$ in S-type granitoid (Tang et al. 2021b). The concentration of P in zircon is an effective fingerprint for identifying zircons derived from S-type granitoid (Burnham and Berry 2012; Zhu et al. 2020), which should be filtered out before applying the Eu/Eu*-in-zircon crustal thickness proxy. In this study, I removed the zircon analyses with a molar P concentration > 15 $\mu mol \cdot g^{-1}$, likely sourced from S-type granitoid (Zhu et al. 2020). I further discarded datasets with $Th/U < 0.1$ to exclude the effects of metamorphic overgrowth (Hoskin and Schaltegger 2003; Tang et al. 2021b). The zircon analysis with high La concentrations (> 1 ppm) was also rejected because high La zircon ($La > 1$ ppm) may reflect

contamination of analyses by inclusions (Tang et al. 2021b). The above screening treatments downsized the dataset to n = 451 (Table S1), which was used to infer the timing of crustal thickening. Sample locations are shown in Fig. 1.

4 Results

The concentration of selected trace elements, Eu/Eu* values, and U–Pb age data of all filtered detrital zircons are presented in Table S1. Figure 2 shows the scatter plot of all filtered detrital zircons Eu/Eu* versus their crystalline ages ($^{206}Pb/^{238}U$ age between 900 and 700 Ma, n = 451). There is no clear trend observable due to scattering in the data. To better understand the Eu/Eu* trend over time, I binned all the filtered data by the age variable into 10 bins of 20 m.y. intervals. There are 54, 53, 53, 92, 79, 39, 36, 27, 13, and 5 detrital zircon grains within the 899–880, 879–860, 859–840, 839–820, 819–800, 799–780, 779–760, 759–740, 739–720 and 719–700 Ma, respectively (see Table S1).

Here, I use age-binned average detrital zircon Eu/Eu* of 20 m.y. intervals to show the Eu/Eu* trend over time. When calculating the age-binned average Eu/Eu* value in each 20 m.y. interval, the following criteria are applied to screen Eu/Eu* values in Table S1 to reduce scatter and bias: (1) when the number of analyses within an interval is limited or there are no obvious outliers, the lowest and highest values are excluded; (2) when the number of analyses within an interval is large, we remove analyses showing the highest 5% and lowest 5% Eu/Eu* values within each 20 m.y. interval. After this screening, 407 out of 451 analyses satisfy the criteria. This screening procedure does not change the overall Eu/Eu* variation pattern.

The overall Eu/Eu* trend implied by the binned averages for every 20 m.y. interval is shown in Fig. 3. This figure displays a decreasing trend of Eu/Eu* from 870 to 790 Ma. Eu/Eu* fluctuates frequently between 790 and 730 Ma without any obvious overall trend. A similar Eu/Eu* pattern, shown in figure S1, was observed when data were plotted as the median Eu/Eu* values for each age group. The empirical equation suggested by (Tang et al. 2021b) was used to calculate the crustal thickness:

$$H = (84.2 \pm 9.2) \times \mathrm{Eu}/\mathrm{Eu}^{*} + (24.5 \pm 3.3).$$

where H is the crustal thickness (in km), and Eu/Eu* is the average Eu/Eu* value in each bin. Calculated age-binned average crustal thickness data are plotted as running averages with two standard errors (Fig. 3a). The age-binned average crustal thickness values during 900–700 Ma estimated using Eu/Eu* in detrital zircon exhibit the same trend of Eu/Eu* values and vary between 40 and 50 km (Fig. 3a).

5 Discussion and conclusions

The variation of crustal thickness through time can provide critical insights into the understanding of tectonic evolution. The central Andes are the type-example of a mountain range constructed by crustal thickening and shortening that result from an accretionary orogen (McGlashan et al. 2008). The crustal thickness beneath the central Andean Plateau is on the order of 60–70 km (Garzione et al. 2008). The Tibetan Plateau, formed from the sequential accretion of continental fragments and island arc terranes beginning during the Paleozoic and culminating during the Cenozoic India–Asia collision, has the thickest crust of 60–80 km (Sundell et al. 2021). The crust of both subduction-related and collision-related mountain belts is observed to thicken significantly. In contrast, the East African rift system, a classic example of a continental rift, has a relatively thinner crustal thickness of about 30 km (Braile et al. 1994).

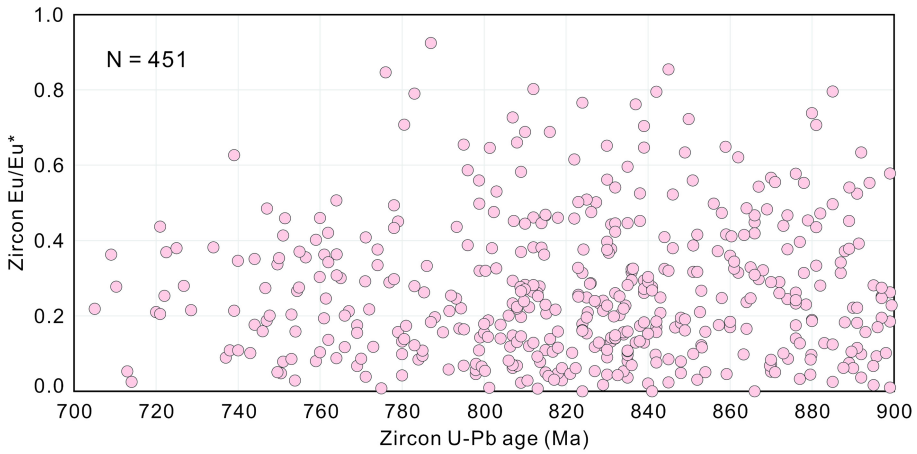

Fig. 2 Scatter plot of zircon Eu/Eu* versus crystallization age (900–700 Ma) for the detrital zircons from central SCB

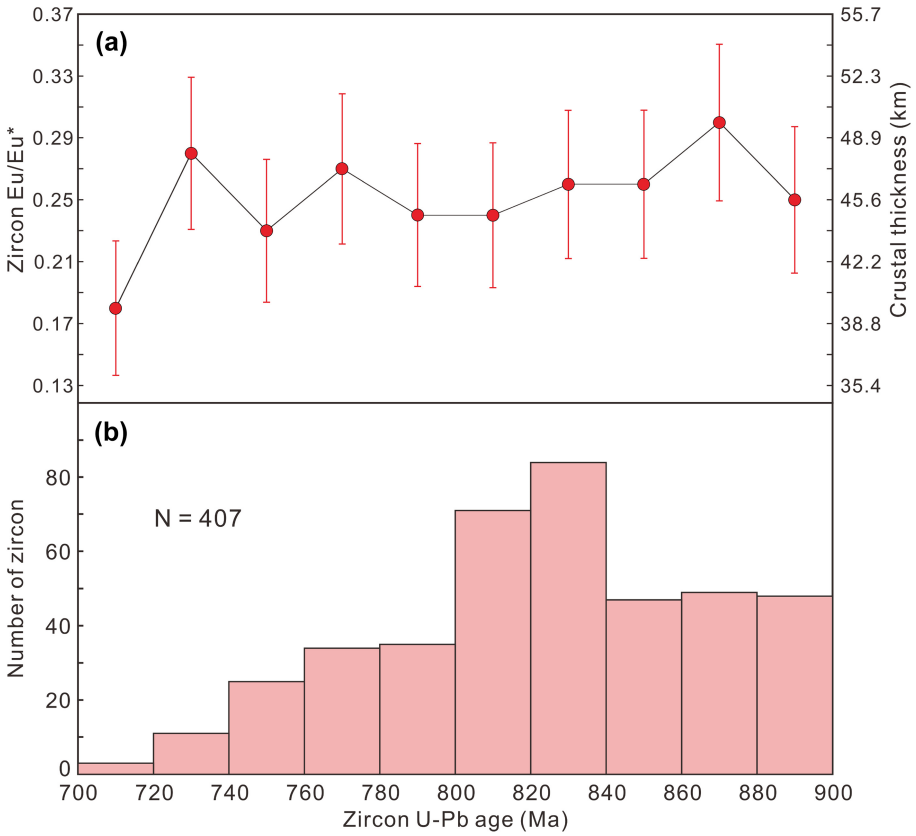

Fig. 3 **a** Crustal thickness evolution of central SCB during 900–700 Ma, reconstructed from Eu/Eu* in detrital zircons. Data are plotted as binned average (bin size 20 million years), with error bars of crustal thickness indicating ± 2 s. **b** Number of detrital zircons within each 20-million-year bin during 900–700 Ma

The reconstructed crustal thickness of South China from age-binned average Eu/Eu* in detrital zircons during 900–700 Ma is on the order of 40–50 km (Fig. 3), consistent with the contemporary mean crustal thickness calculated from global detrital zircon database (Tang et al. 2021a). The calculated crustal thickness during 900–700 Ma is thicker than the modern normal continental thickness, which could be explained by the gradual crust thinning after a continent collision or the limited data size as the robustness of calculated crustal thickness is sensitive to the number of zircon analyses (Tang et al. 2021b). Interpretation of the absolute values of average crustal thickness of South China during 900–700 Ma could be ambiguous, and the trend of the crustal thickness values is more meaningful.

The detrital zircons from South China present a decreasing trend of Eu/Eu* from 870 to 790 Ma (Fig. 3). The crustal thickness is positively correlated with zircon Eu/Eu*, thus the average crustal thickness of South China also shows a decreasing trend from 870 to 790 Ma (Fig. 3) although the calculated crustal thickness values are of large errors. That is to say, the compiled data here do not support a significant crustal thickening event in South China during 870–790 Ma. This observation seems to be at odds with the tectonic model that the amalgamation of the Yangtze and Cathaysia blocks took place through a collisional orogen at ~820 Ma. The other model suggesting an early collision timing (ca. 1000–900 Ma) between the Yangtze and Cathaysia blocks cannot be tested by this study directly. Ca. 1000–900 Ma magmatic rocks are very rare in South China (Li et al. 2014) and detrital zircons of this time interval preserved in the Neoproterozoic sedimentary rocks in South China are usually interpreted to be of exotic origins such as the India block (Cawood et al. 2020). During 790–730 Ma, the calculated average crustal thickness fluctuates frequently without any obvious overall trend. One possible explanation is that there are only a few 790–730 detrital zircon analyses (Fig. 3b), and thus they may not be statistically significant.

The conclusion in this study is based on a limited number of detrital zircons during 900–700 Ma and may be tested when additional detrital zircon data become available. Moreover, the concentration of P used to distinguish zircons derived from S-type granite from those from other types of granite are not available for most of the compiled detrital zircon data. Besides, more zircon proxies such as Al concentration and O–Si isotopes are needed to combine with P concentration to better identify detrital zircons from the S-type granite (Bucholz et al. 2022). Despite these uncertainties, Eu/Eu*-in-zircon-proxy opens the window for extracting crustal thickness information from the extensive detrital zircon archive, which in turn offers a

means of testing tectonic models of South China in the Early-Mid Neoproterozoic. More Neoproterozoic detrital zircon REE, Al-P concentrations, and O–Si isotopic datasets coupled with U–Pb data from South China are needed to better resolve the evolution of crustal thickness and tectonic processes during the Neoproterozoic.

Supplementary Information The online version contains supplementary material available at https://doi.org/10.1007/s11631-023-00605-x.

Acknowledgements This research was financially supported by Nanjing Institute of Geology and Palaeontology, Chinese Academy of Sciences (Grant No. E221110015).

Declarations

Conflict of interest The author declares no conflict of interest.

References

Braile LW, Wang B, Daudt CR, Keller GR, Patel JP (1994) Modeling the 2-D seismic velocity structure across the Kenya rift. Tectonophysics 236:251–269. https://doi.org/10.1016/0040-1951(94)90179-1

Bucholz C, Liebmann J, Spencer CJ (2022) Secular variability in zircon phosphorus concentrations prevents simple petrogenetic classification. Geochem Perspect Lett 24:12–16. https://doi.org/10.7185/geochemlet.2240

Burnham AD, Berry AJ (2012) An experimental study of trace element partitioning between zircon and melt as a function of oxygen fugacity. Geochim Cosmochim Acta 95:196–212. https://doi.org/10.1016/j.gca.2012.07.034

Carrapa B, DeCelles PG, Ducea MN, Jepson G, Osakwe A, Balgord E, Stevens Goddard AL, Giambiagi LA (2022) Estimates of paleo-crustal thickness at Cerro Aconcagua (Southern Central Andes) from detrital proxy-records: implications for models of continental arc evolution. Earth Planet Sci Lett 585:117526. https://doi.org/10.1016/j.epsl.2022.117526

Cawood PA, Wang W, Zhao T, Xu Y, Mulder JA, Pisarevsky SA, Zhang L, Gan C, He H, Liu H, Qi L, Wang Y, Yao J, Zhao G, Zhou M-F, Zi J-W (2020) Deconstructing South China and consequences for reconstructing Nuna and Rodinia. Earth Sci Rev 204:103169. https://doi.org/10.1016/j.earscirev.2020.103169

Charvet J (2013) The Neoproterozoic–Early Paleozoic tectonic evolution of the South China Block: an overview. J Asian Earth Sci 74:198–209. https://doi.org/10.1016/j.jseaes.2013.02.015

Garzione CN, Hoke GD, Libarkin JC, Withers S, MacFadden B, Eiler J, Ghosh P, Mulch A (2008) Rise of the Andes. Science 320:1304–1307. https://doi.org/10.1126/science.1148615

Guo L, Gao R (2018) Potential-field evidence for the tectonic boundaries of the central and western Jiangnan belt in South China. Precambrian Res 309:45–55. https://doi.org/10.1016/j.precamres.2017.01.028

Hoskin PWO, Schaltegger U (2003) The composition of zircon and igneous and metamorphic petrogenesis. Rev Miner Geochem 53:27–62. https://doi.org/10.2113/0530027

Hu F, Ducea MN, Liu S, Chapman JB (2017) Quantifying crustal thickness in continental collisional belts: global perspective and a geologic application. Sci Rep 7:7058. https://doi.org/10.1038/s41598-017-07849-7

Hu F, Wu F, Chapman JB, Ducea MN, Ji W, Liu S (2020) Quantitatively tracking the elevation of the tibetan Plateau since the cretaceous: insights from whole-rock Sr/Y and La/Yb ratios. Geophys Res Lett 47:e2020GL089202. https://doi.org/10.1029/2020GL089202

Jiang W-C, Li H, Mathur R, Wu J-H (2019) Genesis of the giant Shizhuyuan W–Sn–Mo–Bi–Pb–Zn polymetallic deposit, South China: constraints from zircon geochronology and geochemistry in skarns. Ore Geol Rev 111:102980. https://doi.org/10.1016/j.oregeorev.2019.102980

Jiang W-C, Li H, Turner S, Zhu D-P, Wang C (2020) Timing and origin of multi-stage magmatism and related W–Mo–Pb–Zn–Fe–Cu mineralization in the Huangshaping deposit, South China: an integrated zircon study. Chem Geol 552:119782. https://doi.org/10.1016/j.chemgeo.2020.119782

Kong DX (2022) Tracing the effects of fO_2, pressure and H_2O on the ore-forming magmas: perspective from zircon REE composition. J Asian Earth Sci 237:105354. https://doi.org/10.1016/j.jseaes.2022.105354

Kou C, Liu Y, Huang H, Li T, Ding X, Zhang H (2018) The neoproterozoic arc-type and OIB-type mafic-ultramafic rocks in the western Jiangnan Orogen: implications for tectonic settings. Lithos 312–313:38–56. https://doi.org/10.1016/j.lithos.2018.05.004

León S, Monsalve G, Bustamante C (2021) How much did the Colombian Andes rise by the collision of the Caribbean Oceanic Plateau? Res Lett Geophys. https://doi.org/10.1029/2021GL093362

Li Z-X, Li X, Zhou H, Kinny PD (2002) Grenvillian continental collision in south China: new SHRIMP U–Pb zircon results and implications for the configuration of Rodinia. Geology 30:163. https://doi.org/10.1130/0091-7613(2002)030<0163:GCCISC>2.0.CO;2

Li W-X, Li X-H, Li Z-X, Lou F-S (2008a) Obduction-type granites within the NE Jiangxi Ophiolite: implications for the final amalgamation between the Yangtze and Cathaysia Blocks. Gondwana Res 13:288–301. https://doi.org/10.1016/j.gr.2007.12.010

Li Z-X, Bogdanova SV, Collins AS, Davidson A, De Waele B, Ernst RE, Fitzsimons ICW, Fuck RA, Gladkochub DP, Jacobs J, Karlstrom KE, Lu S, Natapov LM, Pease V, Pisarevsky SA, Thrane K, Vernikovsky V (2008b) Assembly, configuration, and break-up history of Rodinia: a synthesis. Precambrian Res 160:179–210. https://doi.org/10.1016/j.precamres.2007.04.021

Li X-H, Li W-X, Li Z-X, Lo C-H, Wang J, Ye M-F, Yang Y-H (2009) Amalgamation between the Yangtze and Cathaysia blocks in South China: Constraints from SHRIMP U–Pb zircon ages, geochemistry and Nd–Hf isotopes of the Shuangxiwu volcanic rocks. Precambrian Res 174:117–128. https://doi.org/10.1016/j.precamres.2009.07.004

Li W-X, Li X-H, Li Z-X (2010) Ca. 850 Ma bimodal volcanic rocks in northeastern Jiangxi Province, South China: initial extension during the breakup of Rodinia? Am J Sci 310:951–980. https://doi.org/10.2475/09.2010.08

Li X-H, Li Z-X, Li W-X (2014) Detrital zircon U–Pb age and Hf isotope constrains on the generation and reworking of precambrian continental crust in the Cathaysia Block, South China: a synthesis. Gondwana Res 25:1202–1215. https://doi.org/10.1016/j.gr.2014.01.003

Lieu WK, Stern RJ (2019) The robustness of Sr/Y and La/Yb as proxies for crust thickness in modern arcs. Geosphere 15:621–641. https://doi.org/10.1130/GES01667.1

Loader MA, Wilkinson JJ, Armstrong RN (2017) The effect of titanite crystallisation on Eu and Ce anomalies in zircon and its implications for the assessment of porphyry Cu deposit fertility.

Earth Planet Sci Lett 472:107–119. https://doi.org/10.1016/j.epsl.2017.05.010

Lu K, Mitchell RN, Yang C, Zhou J-L, Wu L-G, Wang X-C, Li X-H (2022) Widespread magmatic provinces at the onset of the Sturtian snowball Earth. Earth Planet Sci Lett 594:117736. https://doi.org/10.1016/j.epsl.2022.117736

Luffi P, Ducea MN (2022) Chemical mohometry: assessing crustal thickness of ancient orogens using geochemical and isotopic data. Rev Geophys. https://doi.org/10.1029/2021RG000753

Lyu P-L, Li W-X, Wang X-C, Pang C-J, Cheng J-X, Li X-H (2017) Initial breakup of supercontinent Rodinia as recorded by ca 860–840 Ma bimodal volcanism along the southeastern margin of the Yangtze Block, South China. Precambrian Res 296:148–167. https://doi.org/10.1016/j.precamres.2017.04.039

McGlashan N, Brown L, Kay S (2008) Crustal thickness in the central Andes from teleseismically recorded depth phase precursors. Geophys J Int 175:1013–1022. https://doi.org/10.1111/j.1365-246X.2008.03897.x

Meng L, Li Z-X, Chen H, Li X-H, Zhu C (2015) Detrital zircon U–Pb geochronology, Hf isotopes and geochemistry constraints on crustal growth and mesozoic tectonics of southeastern China. J Asian Earth Sci 105:286–299. https://doi.org/10.1016/j.jseaes.2015.01.015

Park Y, Swanson-Hysell NL, Xian H, Zhang S, Condon DJ, Fu H, Macdonald FA (2021) A consistently high-latitude South China from 820 to 780 Ma: implications for Exclusion from Rodinia and the feasibility of large-scale true polar wander. J Geophys Res Solid Earth 126:1–29. https://doi.org/10.1029/2020JB021541

Profeta L, Ducea MN, Chapman JB, Paterson SR, Gonzales SMH, Kirsch M, Petrescu L, DeCelles PG (2015) Quantifying crustal thickness over time in magmatic arcs. Sci Rep 5:17786. https://doi.org/10.1038/srep17786

Qi L, Xu Y, Cawood PA, Zhang H, Zhang Z, Du Y (2021) Implications for supercontinent reconstructions of Mid-Late Neoproterozoic volcanic—sedimentary rocks from the Cathaysia Block, South China. Precambrian Res 354:106056. https://doi.org/10.1016/j.precamres.2020.106056

Shu L, Wang J, Yao J (2019) Tectonic evolution of the eastern Jiangnan region, South China: new findings and implications on the assembly of the Rodinia supercontinent. Precambrian Res 322:42–65. https://doi.org/10.1016/j.precamres.2018.12.007

Shu L, Yao J, Wang B, Faure M, Charvet J, Chen Y (2021) Neoproterozoic plate tectonic process and phanerozoic geodynamic evolution of the South China Block. Earth Sci Rev 216:103596. https://doi.org/10.1016/j.earscirev.2021.103596

Song F, Niu Z-J, He Y-Y, Algeo TJ, Yang W-Q (2020) Geographic proximity of Yangtze and Cathaysia blocks during the Late Neoproterozoic demonstrated by detrital zircon evidence. Palaeogeogr Palaeoclimatol Palaeoecol 558:109939. https://doi.org/10.1016/j.palaeo.2020.109939

Sundell K, Laskowski A, Kapp P, Ducea M, Chapman J (2021) Jurassic to Neogene quantitative crustal thickness estimates in Southern Tibet. GSA Today 31:4–10. https://doi.org/10.1130/GSATG461A.1

Tang M, Lee CTA, Costin G, Höfer HE (2019) Recycling reduced iron at the base of magmatic orogens. Earth Planet Sci Lett 528:115827. https://doi.org/10.1016/j.epsl.2019.115827

Tang M, Chu X, Hao J, Shen B (2021a) Orogenic quiescence in Earth's middle age. Science 371:728–731. https://doi.org/10.1126/science.abf1876

Tang M, Ji W-Q, Chu X, Wu A, Chen C (2021b) Reconstructing crustal thickness evolution from europium anomalies in detrital zircons. Geology 49:76–80. https://doi.org/10.1130/G47745.1

Trail D, Bruce Watson E, Tailby ND (2012) Ce and Eu anomalies in zircon as proxies for the oxidation state of magmas. Geochim Cosmochim Acta 97:70–87. https://doi.org/10.1016/j.gca.2012.08.032

Viala M, Hattori K (2021) Hualgayoc mining district, northern Peru: testing the use of zircon composition in exploration for porphyry-type deposits. J Geochem Explor 223:106725. https://doi.org/10.1016/j.gexplo.2021.106725

Wang J, Li Z-X (2003) History of Neoproterozoic rift basins in South China: implications for Rodinia break-up. Precambrian Res 122:141–158. https://doi.org/10.1016/S0301-9268(02)00209-7

Wang X-C, Li X, Li Z-X, Li Q, Tang G-Q, Gao Y-Y, Zhang Q-R, Liu Y (2012) Episodic precambrian crust growth: evidence from U–Pb ages and Hf–O isotopes of zircon in the Nanhua Basin, central South China. Precambrian Res. https://doi.org/10.1016/j.precamres.2011.06.001

Wang X-L, Zhou J-C, Griffin WL, Zhao G, Yu J-H, Qiu J-S, Zhang Y-J, Xing G-F (2014) Geochemical zonation across a Neoproterozoic orogenic belt: isotopic evidence from granitoids and metasedimentary rocks of the Jiangnan orogen, China. Precambrian Res 242:154–171. https://doi.org/10.1016/j.precamres.2013.12.023

Wang W, Liu-Zeng J, Zeng L, Wang, Wenxin, Tang M, Zhang J (2022) Crustal thickness and paleo-elevation in SE Tibet during the Eocene–Oligocene: insights from whole-rock La/Yb ratios. Tectonophysics 839:229523. https://doi.org/10.1016/j.tecto.2022.229523

Wang Y, Zhang Y, Cawood PA, Zhou Y, Zhang F, Yang X, Cui X (2019) Early Neoproterozoic assembly and subsequent rifting in South China: revealed from mafic and ultramafic rocks, central Jiangnan Orogen. Precambrian Res 331:105367. https://doi.org/10.1016/j.precamres.2019.105367

Wu J-H, Li H, Algeo TJ, Jiang W-C, Zhou Z-K (2018) Genesis of the Xianghualing Sn–Pb–Zn deposit, South China: a multi-method zircon study. Ore Geol Rev 102:220–239. https://doi.org/10.1016/j.oregeorev.2018.09.005

Xiong C, Niu Y, Chen H, Chen A, Zhang C, Li F, Yang S, Xu S (2019) Detrital zircon U–Pb geochronology and geochemistry of late neoproterozoic—early Cambrian sedimentary rocks in the Cathaysia Block: constraint on its palaeo-position in Gondwana supercontinent. Geol Mag 156:1587–1604. https://doi.org/10.1017/S0016756819000013

Xu X, Xue D, Li Y, Hu P, Chen N (2014) Neoproterozoic sequences along the Dexing–Huangshan fault zone in the eastern Jiangnan orogen, South China: geochronological and geochemical constrains. Gondwana Res 25:368–382. https://doi.org/10.1016/j.gr.2013.03.020

Xu X, Li Q, Gui L, Zhang X (2018) Detrital zircon U–Pb geochronology and geochemistry of early neoproterozoic sedimentary rocks from the Northwestern Zhejiang Basin, South China. Mar Pet Geol 98:607–621. https://doi.org/10.1016/j.marpetgeo.2018.09.015

Yang C, Li X-H, Wang X-C, Lan Z (2015) Mid-neoproterozoic angular unconformity in the Yangtze Block revisited: insights from detrital zircon U–Pb age and Hf–O isotopes. Precambrian Res 266:165–178. https://doi.org/10.1016/j.precamres.2015.05.016

Yang Y-N, Wang X-C, Li Q-L, Li X-H (2016) Integrated in situ U–Pb age and Hf–O analyses of zircon from Suixian Group in northern Yangtze: new insights into the neoproterozoic low-$\delta^{18}O$ magmas in the South China Block. Precambrian Res 273:151–164. https://doi.org/10.1016/j.precamres.2015.12.008

Yao J, Shu L, Santosh M, Li J (2012) Precambrian crustal evolution of the South China Block and its relation to supercontinent history: constraints from U–Pb ages, Lu–Hf isotopes and REE geochemistry of zircons from sandstones and granodiorite. Precambrian Res. https://doi.org/10.1016/j.precamres.2012.03.009

Yao W-H, Li Z-X, Li W-X, Su L, Yang J-H (2015) Detrital provenance evolution of the ediacaran–silurian Nanhua foreland basin, South China. Gondwana Res 28:1449–1465. https://doi.org/10.1016/j.gr.2014.10.018

Yao J, Shu L, Zhao G, Han Y, Liu Q (2021) Ca. 835–823 Ma doming extensional tectonics in the west Jiangnan accretionary orogenic belt, South China: implication for a slab roll-back event. J Geodyn 148:101879. https://doi.org/10.1016/j.jog.2021.101879

Zeng Y, Xu J, Chen J, Wang B, Huang F (2022) How and how much did Western Central Tibet raise by India–Asia Collision? Res Lett Geophys. https://doi.org/10.1029/2022gl101206

Zhang J, Ye T, Li S, Yuan G, Dai C, Zhang H, Ma Y (2016) The provenance and tectonic setting of the Lower Devonian sandstone of the Danlin formation in southeast Yangtze plate, with implications for the Wuyi–Yunkai orogeny in South China Block. Sediment Geol 346:25–34. https://doi.org/10.1016/j.sedgeo.2016.10.004

Zhang J, Ye T, Dai Y, Chen J, Zhang H, Dai C, Yuan G, Jiang K (2019) Provenance and tectonic setting transition as recorded in the neoproterozoic strata, western Jiangnan Orogen: implications for South China within Rodinia. Geosci Front 10:1823–1839. https://doi.org/10.1016/j.gsf.2018.10.009

Zhang S-B, He Q, Zheng Y-F (2015) Geochronological and geochemical evidence for the nature of the Dongling complex in South China. Precambrian Res 256:17–30. https://doi.org/10.1016/j.precamres.2014.10.013

Zhang Y, Wang Y, Fan W, Zhang A, Ma L (2012) Geochronological and geochemical constraints on the metasomatised source for the neoproterozoic ($\sim$825 Ma) high-mg volcanic rocks from the Cangshuipu area (Hunan Province) along the Jiangnan domain and their tectonic implications. Precambrian Res. https://doi.org/10.1016/j.precamres.2012.07.003

Zhao G, Cawood PA (2012) Precambrian geology of China. Precambrian Res. https://doi.org/10.1016/j.precamres.2012.09.017

Zhao J-H, Zhou M-F, Yan D-P, Zheng J-P, Li J-W (2011) Reappraisal of the ages of neoproterozoic strata in South China: no connection with the Grenvillian orogeny. Geology 39:299–302. https://doi.org/10.1130/G31701.1

Zhao J-H, Li Q-W, Liu H, Wang W (2018) Neoproterozoic magmatism in the western and northern margins of the Yangtze Block (South China) controlled by slab subduction and subduction-transform-edge-propagator. Earth Sci Rev. https://doi.org/10.1016/j.earscirev.2018.10.004

Zheng YF, Gong B, Zhao ZF, Wu YB, Chen FK (2008) Zircon U–Pb age and O isotope evidence for neoproterozoic low-^{18}O magmatism during supercontinental rifting in South China: implications for the snowball earth event. Am J Sci 308:484–516. https://doi.org/10.2475/04.2008.04

Zhou M-F, Yan D-P, Kennedy AK, Li Y, Ding J (2002) SHRIMP U–Pb zircon geochronological and geochemical evidence for neoproterozoic arc-magmatism along the western margin of the Yangtze Block, South China. Earth Planet Sci Lett 196:51–67. https://doi.org/10.1016/S0012-821X(01)00595-7

Zhu DC, Wang Q, Cawood PA, Zhao ZD, Mo XX (2017) Raising the Gangdese Mountains in southern Tibet. J Geophys Res Solid Earth 122:214–223. https://doi.org/10.1002/2016JB013508

Zhu Z, Campbell IH, Allen CM, Burnham AD (2020) S-type granites: their origin and distribution through time as determined from detrital zircons. Earth Planet Sci Lett 536:116140. https://doi.org/10.1016/j.epsl.2020.116140